

Resonant inelastic x-ray scattering study of overdoped $\text{La}_{2-x}\text{Sr}_x\text{CuO}_4$ S. Wakimoto,^{1,2,*} Young-June Kim,^{1,3} Hyunkyung Kim,¹ H. Zhang,¹ T. Gog,⁴ and R. J. Birgeneau^{1,5}¹Department of Physics, University of Toronto, Toronto, Ontario, Canada M5S 1A7²Advanced Science Research Center, Japan Atomic Energy Research Institute, Tokai, Ibaraki 319-1195, Japan³Department of Physics, Brookhaven National Laboratory, Upton, New York 11973, USA⁴CMC-CAT, Advanced Photon Source, Argonne National Laboratory, Argonne, Illinois 60439, USA⁵Department of Physics, University of California, Berkeley, Berkeley, California 94720-7300, USA

(Received 21 June 2005; revised manuscript received 15 September 2005; published 14 December 2005)

Resonant inelastic x-ray scattering (RIXS) at the copper K absorption edge has been performed for heavily overdoped samples of $\text{La}_{2-x}\text{Sr}_x\text{CuO}_4$ with $x=0.25$ and 0.30 . We have observed the charge-transfer and molecular-orbital excitations, which exhibit resonances at incident energies of $E_i=8.992$ and 8.998 keV, respectively. From a comparison with previous results on undoped and optimally doped samples, we determine that the charge-transfer excitation energy increases monotonically as doping increases. In addition, the E_i dependences of the RIXS spectral weight and absorption spectrum exhibit no clear peak at $E_i=8.998$ keV in contrast to results in the underdoped samples. The low-energy (≤ 3 eV) continuum excitation intensity has been studied utilizing the high-energy resolution of 0.13 eV (full width at half maximum). A comparison of the RIXS profiles at $(\pi, 0)$ and (π, π) indicates that the continuum intensity exists even at (π, π) in the overdoped samples, whereas it has been reported only at $(0, 0)$ and $(\pi, 0)$ for the $x=0.17$ sample. Furthermore, we also found an additional excitation on top of the continuum intensity at the (π, π) and $(\pi, 0)$ positions.

DOI: 10.1103/PhysRevB.72.224508

PACS number(s): 74.72.Dn, 78.70.Ck, 74.25.Jb

I. INTRODUCTION

The essential physics of the hole-doped high- T_c cuprates can be described as that of a doped Mott insulator, which exhibits several phases varying from antiferromagnetic insulator to metallic superconductor. The elucidation of the basic physics of these various complicated phases by studying the elementary excitations could yield information essential for uncovering the mechanism of high- T_c superconductivity. Experimental techniques that can probe the charge excitations have been dramatically developed in recent years. In particular, resonant inelastic x-ray scattering (RIXS) in the hard x-ray regime has attracted much attention due to its ability to probe the momentum dependence of the charge excitations. This technique was initially applied to NiO;¹ in that case, a large enhancement of the inelastic signal with incident photon energy was observed near the Ni K edge. More recently, this technique has been applied to various cuprates, including high- T_c materials²⁻¹¹ and other highly correlated electron systems.¹²⁻¹⁴

A recent RIXS study near the Cu K edge in undoped La_2CuO_4 (LCO) has revealed three features in its charge-excitation spectrum.⁵ Two features, labeled A and B, appear at energy transfers $\omega=2.2$ eV and 3.9 eV, respectively; these features show the largest intensity enhancement at an incident photon energy of $E_i=8.991$ keV. The other feature, labeled C, appears at $\omega=7.2$ eV and resonates at the higher incident energy of $E_i=8.998$ keV. Since the resonance energy of the A and B features corresponds to the absorption feature associated with a well-screened state,¹⁵ these two have been attributed to the charge-transfer (CT) excitations from the O $2p$ to the Cu $3d$ upper Hubbard band. On the other hand, the resonance energy of feature C is associated with a poorly screened state, and has been attributed to a molecular-orbital (MO) excitation that involves a transition

between bonding and antibonding states of the Cu $3d$ and O $2p$ orbitals.⁷

Recently, there has been a number of RIXS studies of doped cuprate superconductors.^{6-8,11} For the $\text{La}_{2-x}\text{Sr}_x\text{CuO}_4$ (LSCO) system, Kim *et al.*⁶ showed that the two features of the CT excitations in LCO are also observed for $x=0.05$, but only a single feature is observed at ~ 4 eV for $x=0.17$. In addition, a continuumlike excitation appears for $x=0.17$ below the charge-transfer excitation energy ($\omega < 2$ eV) at the zone center $(0, 0)$ and at the zone boundary $(\pi, 0)$.⁶ The zone center result is consistent with optical measurements, which show a transfer of the spectral weight from the CT excitation to lower energies.¹⁶ For the MO excitation, the excitation energy increases with doping.⁷ This was attributed to the decreased Cu-O distance in doped samples, which leads to an increased energy splitting between the bonding and antibonding molecular orbitals due to the increased $p-d$ hybridization.

Although measurements have been carried out for underdoped and optimally doped samples, the overdoped region has not yet been studied with RIXS. Such studies should yield important insights into the nature of the charge excitations observed with the RIXS technique. We note that thus far LSCO appears to be the only high- T_c system where large, high-quality heavily overdoped crystals are available. In this paper, we report RIXS results for overdoped LSCO with $x=0.25$ and 0.30 ; the primary purpose of this study is to elucidate the evolution of the charge excitations in the overdoped region. We find that the CT and MO excitations in the overdoped compounds exhibit resonantly enhanced intensity over a broader range of incident energies than those of an optimally doped and undoped (parent) compound. We also observe that the near-edge x-ray-absorption spectrum exhibits a feature associated with the well screened final state,

which is well defined similar to its counterpart in underdoped samples. On the other hand, we do not find a well-defined peak corresponding to the poorly screened final state. Profiles measured utilizing a high energy resolution spectrometer configuration indicate that the continuum excitation exists below 3 eV at (π, π) in addition to the $(0, 0)$ and $(\pi, 0)$ positions. On top of the continuum intensity, we observed an additional excitation at $\omega \sim 1.8$ eV, which exhibits resonantly enhanced intensity around $E_i \sim 8.993$ keV.

The paper is organized as follows. Section II describes the experimental details. The CT and MO excitations measured with a conventional RIXS setup are presented in Sec. III, while a detailed study of the continuum intensity below 3 eV using the high-resolution setup is reported in Sec. IV. Finally, the results are summarized in Sec. V. Since the results for the $x=0.25$ and 0.30 crystals are quantitatively similar, we do not distinguish between these two samples in our discussion unless there is a special need.

II. EXPERIMENTAL DETAILS

Single crystals of LSCO with $x=0.25$ and 0.30 for the RIXS measurements were grown by the traveling-solvent floating-zone (TSFZ) method in the same manner as those used for neutron-scattering experiments.^{17,18} The grown crystal rods have a typical size of 6 mm diam and 80 mm in length; they were cut into pieces 5 mm \times 4 mm \times 1 mm along the tetragonal a , c , and b directions, respectively, and annealed at 850 °C for 12 h in flowing oxygen to compensate for oxygen deficiencies. The temperature dependence of the superconducting shielding fraction determined by magnetization measurements shows that the $x=0.25$ sample has $T_c=15$ K, whereas the $x=0.30$ sample shows no bulk superconductivity down to 2 K. The ac surfaces, which the x-ray beams in the RIXS experiments are incident upon, were polished using a 1 μ m grit size.

The RIXS experiments were performed at the undulator beam line 9IDB at the Advanced Photon Source at Argonne National Laboratory. For the measurements of the CT and MO excitations, we used the Si (333) reflection from the double-bounce main monochromator, together with a spherical Ge(733) analyzer with 1 m radius of curvature. This setup gives an instrumental energy resolution of 0.4 eV full width at half maximum (FWHM). For the measurement of the continuum intensity below 3 eV, a Si(444) channel-cut secondary monochromator was used in addition to a Si(111) primary monochromator. A spherical Ge(733) analyzer with a 2 m radius of curvature was also utilized. This spectrometer configuration yielded a net energy resolution of 0.13 eV (FWHM). More technical details of the finer resolution setup has been reported in Ref. 19.

The energy resolution has been measured by scanning an incoherent background signal along the energy direction. For the finer resolution setup, we cooled the samples down to 9 K by a closed-cycle refrigerator to reduce a possible phonon contribution to the elastic background intensity. However, we found that the elastic peak width along the energy direction does not show clear temperature dependence. Thus, we conclude no phonon effect on the elastic peak.

For all measurements, the scattering plane was vertical and the polarization of the incident x-ray was fixed along the c -axis. Typical scans were performed by counting for 2 min at each data point, and the counts were normalized to monitor counts corresponding to 1 s. In our analysis, we have used the following background subtraction and normalization method. The largest source of background arises from the contribution of the elastic ($\omega=0$) intensity. The energy gain ($\omega < 0$) side spectrum is expected to represent purely background intensity, since the detailed balance factor at this temperature and energy scale vanishes. Therefore, the background subtracted intensity can be written as $D(\omega)=I(\omega)-I(-\omega)$ ($\omega > 0$), where $I(\omega)$ is the raw intensity, assuming that the elastic background is symmetric in ω . Unless noted otherwise, we used the intensity of the Cu $K\beta_5$ emission line as a normalization factor, since this emission intensity is expected to be proportional to the sample volume probed.

At last, throughout this paper, we use tetragonal notation with $a=3.77$ Å along the Cu-O-Cu direction, corresponding to $a^*=1.67$ Å⁻¹.

III. CHARGE TRANSFER AND MOLECULAR ORBITAL EXCITATIONS

First, we present the experimental results for the main spectral features, which correspond to the CT and the MO excitations. Figure 1 shows the evolution of the RIXS spectra as a function of the incident energy E_i near the Cu K edge at the positions $Q=(3.05, 0)$ corresponding to a position near the zone center $q=(0.1\pi, 0)$ and $Q=(2.5, 0)$ corresponding to the zone boundary position $q=(\pi, 0)$. Unfortunately, the zone center $(3, 0, 0)$ position is contaminated at $\omega=0$ presumably by the tails of the Bragg peaks at $(3, 0, 1)$ and $(3, 0, \bar{1})$, so that the data have been obtained at positions slightly away from the zone center. However, a relatively high elastic intensity remains at $(0.1\pi, 0)$, producing a broader tail than that at $(\pi, 0)$. Nevertheless, a similar incident energy dependence of the RIXS spectra is observed at both positions with a CT excitation around 4 eV and the MO excitation around 8 eV, exhibiting resonance enhancements at $E_i \sim 8.992$ keV and ~ 8.998 keV, respectively.

To study any possible change of the RIXS spectra as a function of momentum and doping, the spectral weight has been calculated by simply summing up the background subtracted and normalized intensity between 2 and 12 eV. Spectral weights so obtained for the data at $(0.1\pi, 0)$ and $(\pi, 0)$ are shown in Fig. 2(a) by circles and squares, respectively. Although the (near) zone center data show smaller spectral weights, the E_i dependence appears to be very similar at both positions. This is more clearly seen in Fig. 2(b), which shows the E_i dependences of the spectral weights normalized to their maximum values. Thus, although the excitation energies are slightly different at different q positions as shown in Fig. 1, the resonance behavior is similar.

We observe that the spectral weight does not show a well-defined peak at $E_i \sim 8.998$ keV, which is the MO excitation resonance energy, whereas the spectral weight has a peak at $E_i \sim 8.992$ keV, the CT excitation resonance energy. We also

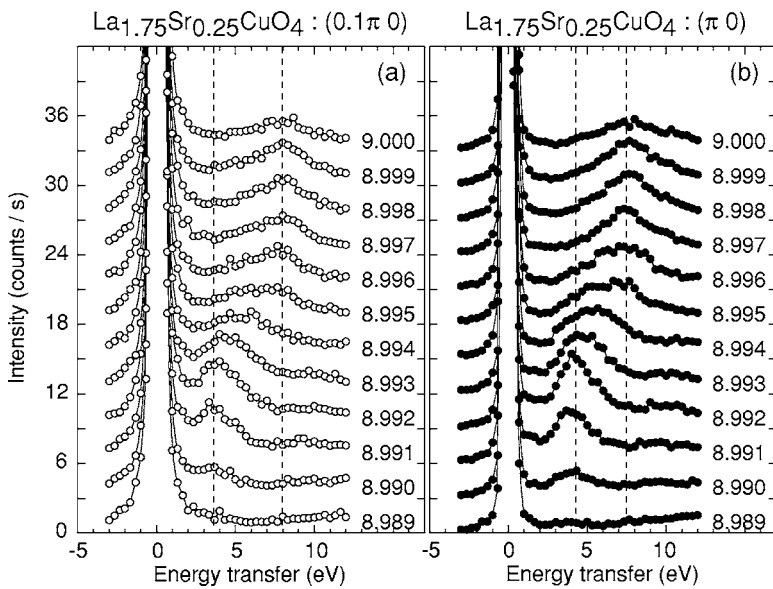


FIG. 1. E_i variation of the room-temperature RIXS spectra of the $x=0.25$ sample at (a) a position near the zone center ($0.1\pi 0$) and (b) zone boundary ($\pi 0$). These are measured at $Q = (3.05, 0, 0)$ and $(2.5, 0.5, 0)$, respectively. The data are shifted vertically for clarity. Dashed lines represent energies of the CT and the MO excitations.

found that the x-ray-absorption spectrum shown in Fig. 2(c), which is measured by monitoring the intensity of Cu $K\beta_5$ line at $E_f=8.973$ keV, does not exhibit a well-defined peak associated with the so-called poorly screened state around 8.998 keV. This result should be contrasted with the results in the undoped samples. Figure 2(d) shows the spectral weight of La_2CuO_4 calculated in the same manner using the data reported in Ref. 5. It is clearly seen that the spectral weight of La_2CuO_4 has two well-defined peaks at the ener-

gies where the CT and the MO excitations resonate. Consistent with this, the absorption spectrum of La_2CuO_4 also has the well-defined peaks for both well-screened and poorly screened states as shown in Fig. 2(e).⁵ Since such a two-peak structure has also been observed for the $x=0.17$ sample,⁶ the disappearance of the higher energy peak in the absorption spectrum and the broad nature of the RIXS spectral weight distribution seem to be characteristic of overdoped metallic samples.

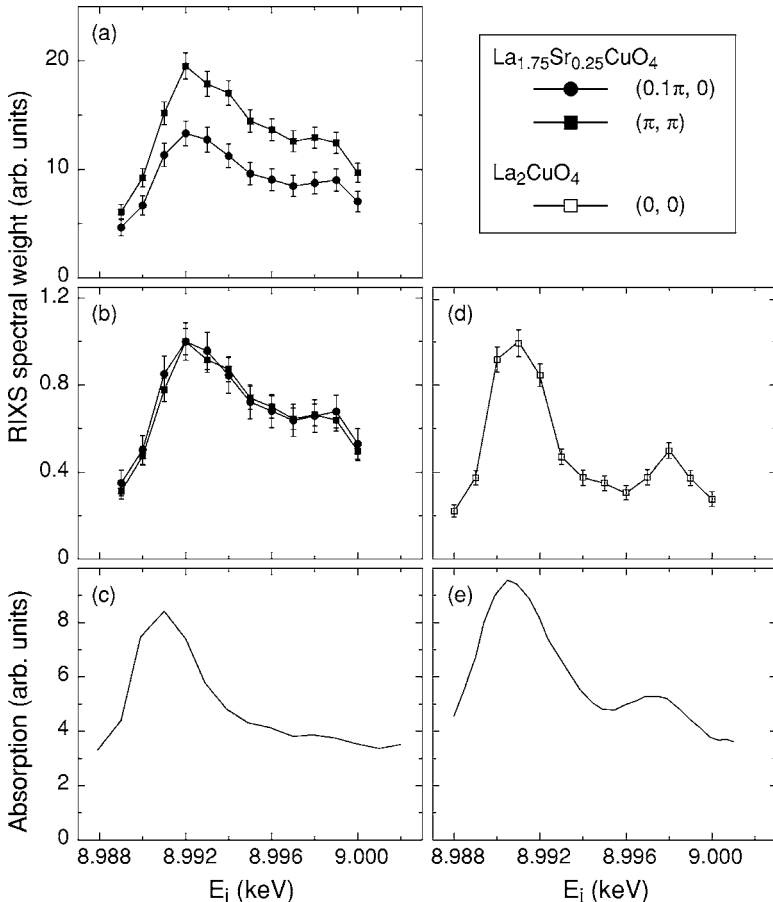


FIG. 2. (a) RIXS spectral weights for the $x=0.25$ sample as a function of E_i . The spectral weights are normalized to the effective volumes estimated from the Cu- $K\beta_5$ intensity. (b) RIXS spectral weights normalized to the maximum value. For (a) and (b), the squares and circles represent data at $(0.1\pi 0)$ and $(\pi 0)$, respectively. (d) shows spectral weight of the parent material La_2CuO_4 calculated from the data reported in Fig. 1(a) of Ref. 5. The data are normalized to the maximum value. (c) and (e) indicate the absorption of $x=0.25$ and pure samples, respectively, measured by monitoring the Cu- $K\beta_5$ intensity. The data of (e) is referred from Fig. 1(b) of Ref. 5. Error bars in (a), (b), and (d) result from a summation of the statistical errors of summed data points.

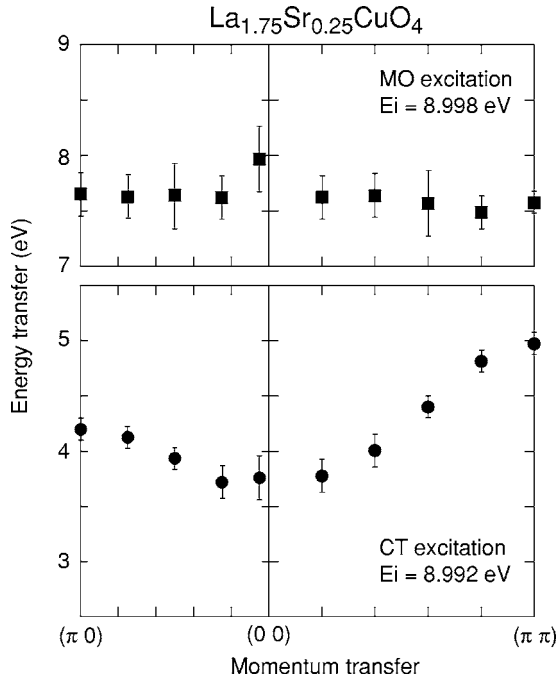


FIG. 3. Dispersion relation of the MO excitation (upper) measured with $E_i=8.998$ keV and the CT excitation (lower) measured with $E_i=8.992$ keV for $x=0.25$. Error bars are estimated from a simple fit to a Lorentzian function.

The dispersions of the CT and the MO excitations have been studied by collecting the RIXS spectra at fixed $E_i=8.992$ keV and 8.998 keV at several q positions between $(3, 0)$ and $(2.5, 0)$, and between $(3, 0)$ and $(2.5, 0.5)$. The data have been fitted by a Lorentzian function with a sloping background to determine the excitation energies. The dispersions so obtained are shown in Fig. 3. The CT excitation appears at 3.7 eV at the zone center and reaches 4.2 eV at $(\pi 0)$ and 5 eV at $(\pi \pi)$. This dispersion is qualitatively similar to that observed in the $x=0.17$ sample.⁶ The actual profiles, however, show systematic changes with increasing hole concentration. The left panel of Fig. 4 indicates profiles of the CT peak for $x=0, 0.17$ (from Refs. 5 and 6) and 0.30. To compare the CT peak itself, the intensity is normalized to the CT peak intensity. It may be clearly seen that the CT peak shifts its weight to higher energy with increasing doping at all q positions. This is consistent with an increase of the CT gap with doping predicted by Tsutsui *et al.*²⁰ and agrees quantitatively with their numerical calculations.^{21,22} The large value of this shift (~ 1 eV) is somewhat surprising, given that the chemical potential shift due to the hole doping observed in photoemission experiments is <0.5 eV.²³ However, the upper Hubbard band shifts to higher energy as holes are doped.²² This combined effect of the chemical potential shift and the shift of the unoccupied band seems to contribute to the large overall shift of the CT feature.

It is also interesting to note that the large shift of the CT peak energy in the overdoped regime may imply a large overlap of the O $2p$ and the lower Hubbard Cu $3d$ bands, resulting in the existence of partially doped holes with Cu $3d$ character in the overdoped regime. This, in turn, would suppress magnetic correlations as reported by recent neutron-

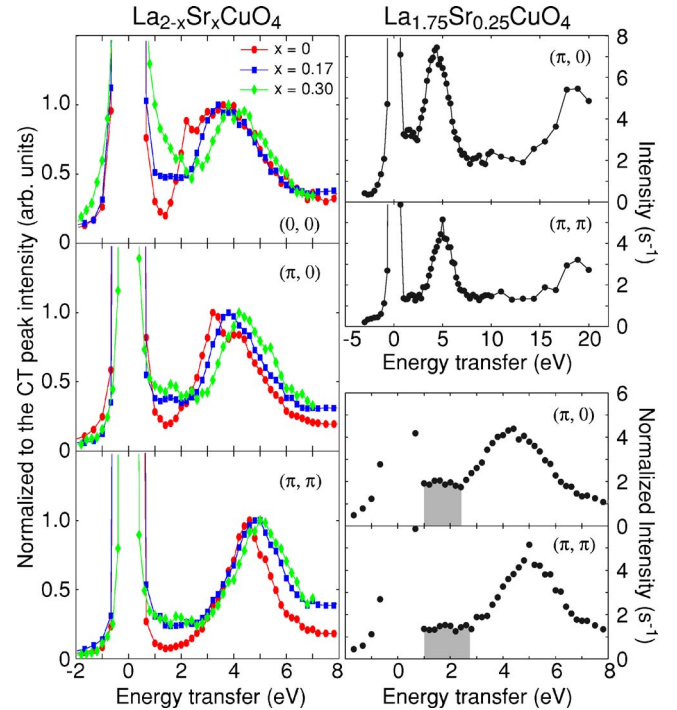


FIG. 4. (Color online) The left panel shows a comparison of the RIXS spectra for $x=0, 0.17$, and 0.30 at three different q positions. The data for $x=0$ and 0.17 are referred from Refs. 5 and 6. The profiles are normalized to the CT peak intensity. The data for $x=0.30$ were taken utilizing the fine energy resolution setup. The right panel shows the RIXS spectra for $x=0.25$ with data as measured (top) and normalized to the Cu $K\beta_5$ intensity (bottom).

scattering measurements of the overdoped samples.^{17,18} However, detailed numerical calculations are necessary to draw any firm conclusions.

The nature of the MO excitation also appears to differ from that in the $x=0.17$ sample.⁷ Although the zone boundary has a lower excitation energy than the zone center, as is the case for $x=0.17$, the dispersion of the overdoped sample is flat in the large q region as shown in Fig. 3. As discussed in Ref. 7, the energy and the dispersion of the MO excitation increases as the Cu-O distance decreases, and concomitantly, the hybridization between the Cu $3d_{x^2-y^2}$ and the O $2p_\sigma$ orbitals becomes stronger. The excitation energy of 7.6 eV at $(\pi 0)$ is very close to that of the $x=0.17$ sample, which has the same Cu-O distance as the $x=0.25$ sample, and, moreover, if we define the dispersion as the difference between the energies at $(\pi 0)$ and $(0 0)$, the overall dispersion of ~ 0.4 eV of the present sample is similar to that of the $x=0.17$ sample (~ 0.5 eV).

IV. LOW-ENERGY EXCITATION

The plots on the left side of Fig. 4 show clear evidence for the appearance of a low energy excitation below the CT peak for the doped samples. Although the excitation spectrum around 1 eV for the undoped sample decreases to the background level (intensity at $\omega=-1$ eV), the intensity at 1 eV remains well above the background in the doped samples. As

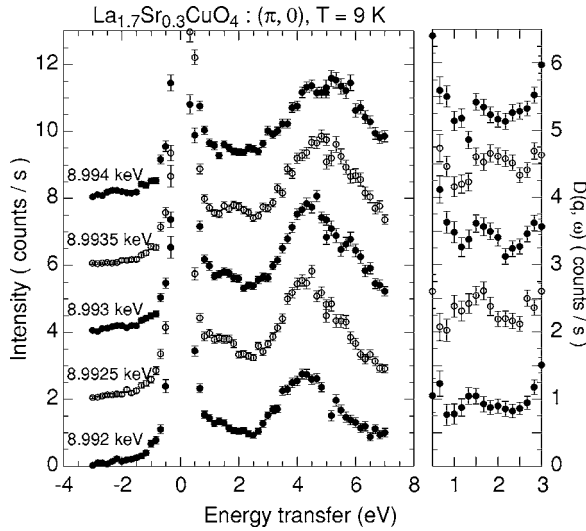


FIG. 5. (Left) RIXS spectra of the $x=0.30$ sample at $(\pi, 0)$ at various E_i at 9 K. Each spectrum is shifted by two counts for clarity. (Right) The differential intensity $D(q, \omega)$ derived by subtracting the energy gain side intensity as a background from the energy loss side. The data are shifted by one count each.

reviewed in Sec. I, Kim *et al.*⁶ have observed that the continuum intensity at low energy ($1 \sim 2$ eV) exists at $(0, 0)$ and at $(\pi, 0)$, but not at (π, π) . To test this in the overdoped sample, we have compared the RIXS spectra for $x=0.25$ at $(\pi, 0)$ and (π, π) . The top-right panel of Fig. 4 shows the as-measured data of RIXS spectra taken with $E_i = 8.992$ keV, including the peak around 19 eV due to the Cu $K\beta_5$ fluorescence emission. The bottom-right panel shows the same spectrum after normalization using the Cu $K\beta_5$ intensity. Both spectra exhibit a constant intensity between 1 and 3 eV as shown by the shaded area, although the continuum intensity at the (π, π) position appears to be smaller than that at $(\pi, 0)$. Thus, the data are suggestive of the existence of the continuum excitation even at (π, π) in the overdoped samples.

We have also measured the RIXS spectra for $x=0.30$ at 9 K utilizing the high resolution instrumentation (~ 0.13 eV) which enables us to study the detailed structure of the continuum excitation. Figure 5 shows the evolution of the RIXS spectra as a function of E_i between 8.992 and 8.994 keV at $(\pi, 0)$. It appears that there is a small peak on top of the continuum intensity at ~ 1.5 eV resonating in the range of $8.9925 \leq E_i \leq 8.9935$ keV. This may be more clearly seen in the right panel of the figure, where the background-subtracted spectra are plotted on a different scale to emphasize the continuum region. The data below 1 eV have a large ambiguity due to the tail of the elastic peak, while the increase of $D(\omega)$ above 2.5 eV is due to the CT peak. A peak at 1.5 eV is, nevertheless, clear in the range of $8.992 \leq E_i \leq 8.993$ keV.

Similar features have been found at the (π, π) position. Figure 6 shows plots analogous to those in Fig. 5 for (π, π) . In the right panel, the profile at $E_i = 8.993$ keV exhibits a peak of 0.5 counts/s appearing around $\omega = 1.8$ eV on top of the continuum intensity of 1 count/s, whereas the data at

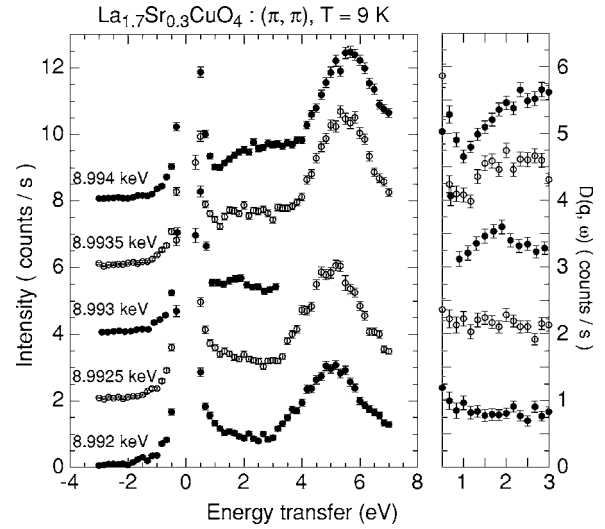


FIG. 6. Analogous plots to Fig. 5 for the RIXS spectra at (π, π) .

$E_i = 8.992$ and 8.9925 keV show only a flat continuum intensity. As E_i increases to 8.994 keV, the peak appears to become broader and larger, and seems to shift to higher energy.

We have studied the q dependence of this excitation around (π, π) with fixed E_i at 8.993 eV. Figure 7 shows the background-subtracted and normalized RIXS intensity

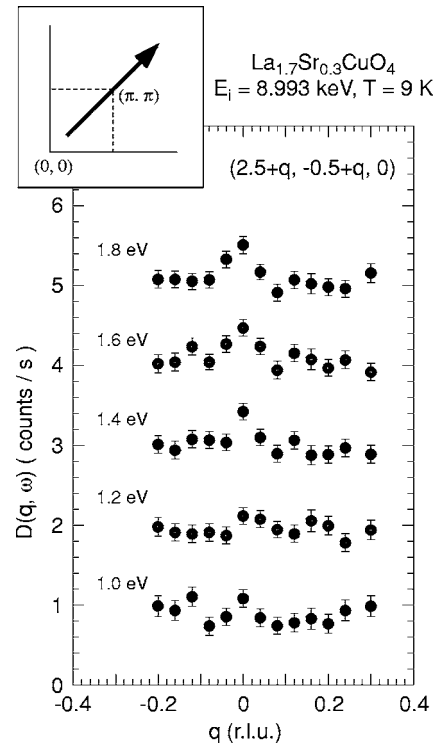


FIG. 7. q -dependence of the RIXS intensity of the $x=0.30$ sample for $1 \leq \omega \leq 1.8$ eV. The data are derived by normalizing to the intensity at $\omega=0$ eV after subtracting the energy gain side intensity as a background. Error bars result from a summation of the statistical errors of the energy loss signal and the energy gain background. The data are shifted vertically for clarity. The scanning direction is shown by an arrow in the inset.

$D(q, \omega)$ at $1.0 \leq \omega \leq 1.8$ eV along the $(2.5+q, -0.5+q, 0)$ direction, which is equivalent to the trajectory in a reduced momentum space shown by an arrow in the inset. It is evident that a peak develops at (π, π) with increasing energy transfer and it reaches an intensity of ~ 0.5 counts/s at 1.8 eV on top of the q -independent continuum intensity of 1 count/s, consistent with the data for $E_i = 8.993$ eV in Fig. 6.

It is an open question what the origin of this excitation is. From a consideration of the excitation energy of this feature, a possible origin is the local dd excitation, which has been observed around 1.5 eV.^{24,25} However, more detailed measurements are necessary to draw definitive conclusions.

V. CONCLUDING REMARKS

We have studied heavily overdoped LSCO with $x=0.25$ and 0.30 using the resonant inelastic x-ray-scattering technique near the Cu K edge. We observe several features of the charge-transfer and molecular-orbital excitations in these materials. First, the resonance behavior in this overdoped sample appears to be broader in incident photon energy than that of the undoped parent material. Furthermore, in the absorption spectra of the overdoped samples, the peak corresponding to the poorly screened state is damped. This presumably is related to the metallic nature of the overdoped samples and the better screening due to mobile charge carriers.

Second, we found that the CT peak energy increases with doping x . This agrees with the prediction of an increase of the CT gap energy with increasing x and, specifically, the numerical calculations of Tsutsui *et al.*^{20,21} and Tsutsui²².

Our study of the low-energy excitations has shown that the continuum intensity appears at all momentum transfers for the overdoped samples. From detailed measurements utilizing the high-energy resolution of 0.13 eV, we observed an additional excitation on the continuum intensity at (π, π) and $(\pi, 0)$, which shows resonantly enhanced intensity at $E_i \sim 8.993$ keV. It will be important to study the dispersion of this feature, as well as to determine whether or not this excitation exists in the samples with lower doping to elucidate the origin of this excitation.

ACKNOWLEDGMENTS

The authors thank D. Casa, D. Ellis, J. P. Hill, K. Tsutsui, C. T. Venkataraman, and K. Yamada for invaluable discussions. The work at the University of Toronto is part of the Canadian Institute of Advanced Research and supported by Natural Science and Engineering Research Council of Canada. The work at BNL is supported by the U. S. Department of Energy, Division of Material Science, under Contract No. DE-AC02-98CH10886. The APS is supported by the U. S. Department of Energy, Basic Energy Sciences, Office of Science, under Contract No. W-31-109-Eng-38.

*Corresponding author.

Electronic address: swakimoto@neutrons.tokai.jaeri.go.jp

- ¹C.-C. Kao, W. A. L. Caliebe, J. B. Hastings, and J. M. Gillet, *Phys. Rev. B* **54**, 16361 (1996).
- ²J. P. Hill, C.-C. Kao, W. A. L. Caliebe, M. Matsubara, A. Kotani, J. L. Peng, and R. L. Greene, *Phys. Rev. Lett.* **80**, 4967 (1998).
- ³P. Abbamonte, C. A. Burns, E. D. Isaacs, P. M. Platzman, L. L. Miller, S. W. Cheong, and M. V. Klein, *Phys. Rev. Lett.* **83**, 860 (1999).
- ⁴M. Z. Hasan, E. D. Isaacs, Z.-X. Shen, L. L. Miller, K. Tsutsui, T. Tohyama, and S. Maekawa, *Science* **288**, 1811 (2000).
- ⁵Y. J. Kim, J. P. Hill, C. A. Burns, S. Wakimoto, R. J. Birgeneau, D. Casa, T. Gog, and C. T. Venkataraman, *Phys. Rev. Lett.* **89**, 177003 (2002).
- ⁶Y.-J. Kim, J. P. Hill, S. Komiya, Y. Ando, D. Casa, T. Gog, and C. T. Venkataraman, *Phys. Rev. B* **70**, 094524 (2004).
- ⁷Y.-J. Kim, J. P. Hill, G. D. Gu, F. C. Chou, S. Wakimoto, R. J. Birgeneau, S. Komiya, Y. Ando, N. Motoyama, K. M. Kojima, S. Uchida, D. Casa, and T. Gog, *Phys. Rev. B* **70**, 205128 (2004).
- ⁸M. Z. Hasan, Y. Li, D. Qian, Y.-D. Chuang, H. Eisaki, S. Uchida, Y. Koga, T. Sasagawa, and H. Takagi, cond-mat/0406654 (unpublished).
- ⁹K. Ishii, K. Tsutsui, Y. Endoh, T. Tohyama, K. Kuzushita, T. Inami, K. Ohwada, S. Maekawa, T. Masui, S. Tajima, Y. Murakami, and J. Mizuki, *Phys. Rev. Lett.* **94**, 187002 (2005).
- ¹⁰K. Ishii, K. Tsutsui, Y. Endoh, T. Tohyama, S. Maekawa, M. Hoesch, K. Kuzushita, M. Tsubota, T. Inami, J. Mizuki, Y. Mu-

- rakami, and K. Yamada, *Phys. Rev. Lett.* **94**, 207003 (2005).
- ¹¹L. Lu, G. Chabot-Couture, X. Zhao, J. N. Hancock, N. Kaneko, O. P. Vajk, G. Yu, S. Grenier, Y. J. Kim, D. Casa, T. Gog, and M. Greven, *Phys. Rev. Lett.* **95**, 217003 (2005).
- ¹²M. Z. Hasan, P. A. Montano, E. D. Isaacs, Z.-X. Shen, H. Eisaki, S. K. Sinha, Z. Islam, N. Motoyama, and S. Uchida, *Phys. Rev. Lett.* **88**, 177403 (2002).
- ¹³Y.-J. Kim, J. P. Hill, F. C. Chou, D. Casa, T. Gog, and C. T. Venkataraman, *Phys. Rev. B* **69**, 155105 (2004).
- ¹⁴Y.-J. Kim, J. P. Hill, H. Benthien, F. H. L. Essler, E. Jeckelmann, H. S. Choi, T. W. Noh, N. Motoyama, K. M. Kojima, S. Uchida, D. Casa, and T. Gog, *Phys. Rev. Lett.* **92**, 137402 (2004).
- ¹⁵C. Li, M. Pompa, A. C. Castellano, S. D. Longa, and A. Bianconi, *Physica C* **175C**, 369 (1991).
- ¹⁶S. Uchida, T. Ido, H. Takagi, T. Arima, Y. Tokura, and S. Tajima, *Phys. Rev. B* **43**, 7942 (1991).
- ¹⁷S. Wakimoto, H. Zhang, K. Yamada, I. Swainson, Hyunkyung Kim, and R. J. Birgeneau, *Phys. Rev. Lett.* **92**, 217004 (2004).
- ¹⁸S. Wakimoto, R. J. Birgeneau, A. Kagedan, Hyunkyung Kim, I. Swainson, K. Yamada, and H. Zhang, *Phys. Rev. B* **72**, 064521 (2005).
- ¹⁹J. P. Hill, D. S. Coburn, Y.-J. Kim, T. Gog, N. Koditwaku, and H. Sinn, *J. Phys. Chem. Solids* (to be published).
- ²⁰K. Tsutsui, T. Tohyama, and S. Maekawa, *Phys. Rev. Lett.* **91**, 117001 (2003).
- ²¹K. Tsutsui, T. Tohyama, and S. Maekawa, *Physica C* **412-414**, 143 (2004).
- ²²K. Tsutsui (private communication).

- ²³A. Ino, T. Mizokawa, A. Fujimori, K. Tamasaku, H. Eisaki, S. Uchida, T. Kimura, T. Sasagawa, and K. Kishio, Phys. Rev. Lett. **79**, 2101 (1997).
- ²⁴Pieter Kuiper, J.-H. Guo, C. Sathe, L.-C. Duda, Joseph Nordgren, J. J. M. Poethuizen, F. M. F. de Groot, and G. A. Sawatzky, Phys. Rev. Lett. **80**, 5204 (1998).
- ²⁵G. Ghiringhelli, N. B. Brookes, E. Annese, H. Berger, C. Dallera, M. Grioni, L. Perfetti, A. Tagliaferri, and L. Braicovich, Phys. Rev. Lett. **92**, 117406 (2004).